154 *Journal of Electrical Engineering & Technology Vol. 6, No. 2, pp. 154~160, 2011*
DOI: 10.5370/JEET.2011.6.2.154

Fundamental Frequency Estimation in Power Systems Using Complex Prony Analysis

Soon-Ryul Nam†, Dong-Gyu Lee*, Sang-Hee Kang*, Seon-Ju Ahn, and Joon-Ho Choi****

Abstract – A new algorithm for estimating the fundamental frequency of power system signals is presented. The proposed algorithm consists of two stages: orthogonal decomposition and a complex Prony analysis. First, the input signal is decomposed into two orthogonal components using cosine and sine filters, and a variable window is adapted to enhance the performance of eliminating harmonics. Then a complex Prony analysis that is proposed in this paper is used to estimate the fundamental frequency by approximating the cosine-filtered and sine-filtered signals simultaneously. To evaluate the performance of the algorithm, amplitude modulation and harmonic tests were performed using simulated test signals. The performance of the algorithm was also assessed for dynamic conditions on a single-machine power system. The Electromagnetic Transients Program was used to generate voltage signals for a load increase and single phase-to-ground faults. The performance evaluation showed that the proposed algorithm accurately estimated the fundamental frequency of power system signals in the presence of amplitude modulation and harmonics.

Keywords: Complex Prony analysis, Frequency estimation, Orthogonal decomposition

1. Introduction

When measuring, controlling, or protecting power systems, accurate estimation of the fundamental frequency of their signals is important. In particular, a real-time accurate estimate of the fundamental frequency is a prerequisite for electrical parameter measurements. This is because various numerical algorithms for electrical parameter measurements are sensitive to frequency variations. Typical examples are algorithms based on discrete Fourier transform (DFT) or least-mean-square (LMS) methods.

Several methods for frequency estimation have been reported in the technical literature [1-19]. Zero-crossing-based techniques are the most widely used methods for frequency estimation [1, 2]. However, they are incapable of making fast estimates using polluted signals, and their performance is sensitive to switching-type transients. The Kalman filter has also been used to estimate power system frequencies [3, 4], but it is sensitive to the initial conditions and its performance is not robust with respect to variations in the internal parameters of the model. A three-phase, phase-locked loop (PLL) provides fast and robust frequency estimates for balanced three-phase systems and has been widely used for frequency estimation [5–7]. However, its performance is prone to error in unbalanced conditions. A variety of approaches, including adaptive neural networks (ANN) [8, 9], least square techniques [10–12], Newton-type algorithms [13], Prony estimation [14], DFTs [15–17], and the maximum likelihood method [18, 19] have also been used to estimate the frequency of power system signals.

This paper presents a new algorithm for frequency estimation that is based on complex Prony analysis. Simulated tests confirm the efficiency and validity of the proposed algorithm for estimating the fundamental frequency, regardless of the amplitude modulation and harmonics. This paper is divided into four parts, including the introduction. Sections 2 and 3 describe the formulation and the simulation results of the proposed algorithm, respectively, and our conclusions are given in Section 4.

2. Frequency Estimation

Assuming that a continuous-time signal, $x(t)$, has a sinusoidal waveform with a amplitude, frequency, and phase of A, f, and θ, respectively,

$$x(t) = A \cdot \cos(2\pi ft + \theta) \tag{1}$$

this can be discretized as

$$x[n] = A \cdot \cos(2\pi \frac{f}{f_0}\frac{n}{N_0} + \theta) = A \cdot \cos(2\pi f \cdot n\Delta t + \theta) \tag{2}$$

where f_0 is the nominal fundamental frequency, N_0 is the number of samples per cycle at f_0, and Δt is the sampling period.

† Corresponding Author: Department of Electrical Engineering, Myongji University, Yongin 449-728, Korea. (ptsouth@mju.ac.kr)
* Department of Electrical Engineering, Myongji University, Yongin 449-728, Korea. (mallow@mju.ac.kr, shkang@mju.ac.kr)
** Department of Electrical Engineering, Chonnam National University, Gwangju 500-757, Korea. (seonjuahn@gmail.com, joono@chonnam.ac.kr)
Received: May 16, 2010; Accepted:November 11, 2010

2.1 Orthogonal Decomposition

The discrete-time signal, $x[n]$, can be decomposed into real and imaginary components, each orthogonal in phase, using cosine and sine filters. Their coefficients are

$$H_{C_0}(k) = \frac{2}{N_0}\cos(2\pi\frac{k}{N_0}) \qquad k = 0, \cdots, N_0 - 1 \quad (3)$$

$$H_{S_0}(k) = \frac{2}{N_0}\sin(2\pi\frac{k}{N_0}) \qquad k = 0, \cdots, N_0 - 1 \quad (4)$$

When the actual fundamental frequency is equal to the nominal fundamental frequency, the cosine and sine filters can eliminate the harmonics from input signals perfectly. However, when the actual fundamental frequency deviates from the nominal fundamental frequency, the ability of the two filters to eliminate the harmonics is reduced. The variable window technique [20] is used to overcome this drawback. The orthogonal decomposition involves adjusting the data window as close to one cycle of the input signal as possible. Since the sampling period is fixed, the cosine and sine filters must have a filtering fundamental frequency that corresponds to an integer multiple value of the sampling period. Therefore, depending on the estimated fundamental frequency, the variable window is adjusted to the nearest possible integer window,

$$H_C(k) = \frac{2}{N_w}\cos(2\pi\frac{k}{N_w}) \qquad k = 0, \cdots, N_w - 1 \quad (5)$$

$$H_S(k) = \frac{2}{N_w}\sin(2\pi\frac{k}{N_w}) \qquad k = 0, \cdots, N_w - 1 \quad (6)$$

where N_w is the nearest possible integer number of samples per cycle at f.

Assuming that the amplitude and phase response of the cosine filter are $|H_C(f)|$ and $\angle H_C(f)$, respectively, applying (5) to $x[n]$ yields the following output, which corresponds to the real component of $x[n]$:

$$x_R[n] = A_R \cdot \cos(2\pi\frac{f}{f_0}\frac{n}{N_0} + \theta_R) \quad (7)$$

where $A_R = A \cdot |H_C(f)|$, $\theta_R = \theta + \angle H_C(f)$.

Similarly, assuming that the amplitude response of the sine filter is $|H_S(f)|$, applying (6) to $x[n]$ yields the following output, which corresponds to the imaginary component of $x[n]$:

$$x_I[n] = A_I \cdot \sin(2\pi\frac{f}{f_0}\frac{n}{N_0} + \theta_R) \quad (8)$$

where $A_I = A \cdot |H_S(f)|$.

Therefore, the orthogonal decomposition can be expressed in the complex form as

$$\mathbf{X}[n] = x_R[n] + j \cdot x_I[n] \quad (9)$$

2.2 Complex Prony Analysis

In order to estimate the fundamental frequency by approximating the real and imaginary components of the orthogonal decomposition simultaneously, a complex Prony analysis is proposed in this paper.

According to the Prony estimation reported in [14], the real component of the orthogonal decomposition can be approximated as

$$x_R[n] = \alpha_1(z_1)^n + \alpha_2(z_2)^n \quad (10)$$

where

$$\alpha_1 = \frac{A_R}{2}e^{j\theta_R}, \ \alpha_2 = \alpha_1^* = \frac{A_R}{2}e^{-j\theta_R},$$
$$z_1 = e^{-\lambda + j2\pi f \cdot \Delta t}, \ z_2 = z_1^* = e^{-\lambda - j2\pi f \cdot \Delta t}.$$

Since the real and imaginary components of orthogonal decomposition have the same phase, θ_R, as shown in (7) and (8), the imaginary component can be approximated as

$$x_I[n] = \beta_1(z_1)^n + \beta_2(z_2)^n \quad (11)$$

where

$$\beta_1 = \frac{A_I}{2}e^{j(\theta_R - \frac{\pi}{2})}, \ \beta_2 = \beta_1^* = \frac{A_I}{2}e^{-j(\theta_R - \frac{\pi}{2})}.$$

Substituting (10) and (11) into (9) yields

$$\begin{aligned}\mathbf{X}[n] &= x_R[n] + j \cdot x_I[n] \\ &= \alpha_1(z_1)^n + \alpha_2(z_2)^n + j \cdot \{\beta_1(z_1)^n + \beta_2(z_2)^n\}\end{aligned} \quad (12)$$

The purpose of a complex Prony analysis is to find the values of α_k, β_k and z_k that satisfy (12). By using (10) and (11), the three successive samples of (12) can be written in matrix form:

$$\begin{bmatrix} x_R[0] & x_I[0] \\ x_R[1] & x_I[1] \\ x_R[2] & x_I[2] \end{bmatrix} = \begin{bmatrix} z_1^0 & z_2^0 \\ z_1^1 & z_2^1 \\ z_1^2 & z_2^2 \end{bmatrix} \cdot \begin{bmatrix} \alpha_1 & \beta_1 \\ \alpha_2 & \beta_2 \end{bmatrix} \quad (13)$$

where z_k are necessarily the solutions of a second-order Eq. with unknown coefficients e_k, and thus satisfy

$$e_0 \cdot z_k^0 + e_1 \cdot z_k^1 - z_k^2 = 0 \quad (14)$$

The application of the coefficients e_k to (13) forms

$$\begin{bmatrix} e_0 \\ e_1 \\ -1 \end{bmatrix}^T \begin{bmatrix} x_R[0] & x_I[0] \\ x_R[1] & x_I[1] \\ x_R[2] & x_I[2] \end{bmatrix} = \begin{bmatrix} e_0 \\ e_1 \\ -1 \end{bmatrix}^T \begin{bmatrix} z_1^0 & z_2^0 \\ z_1^1 & z_2^1 \\ z_1^2 & z_2^2 \end{bmatrix} \cdot \begin{bmatrix} \alpha_1 & \beta_1 \\ \alpha_2 & \beta_2 \end{bmatrix} \quad (15)$$

Some minor calculations give the following Eq.:

$$\begin{bmatrix} e_0 x_R[0] + e_1 x_R[1] - x_R[2] \\ e_0 x_I[0] + e_1 x_I[1] - x_I[2] \end{bmatrix}^T = \begin{bmatrix} e_0 z_1^0 + e_1 z_1^1 - z_1^2 \\ e_0 z_2^0 + e_1 z_2^1 - z_2^2 \end{bmatrix}^T \begin{bmatrix} \alpha_1 & \beta_1 \\ \alpha_2 & \beta_2 \end{bmatrix} \quad (16)$$

Substituting (14) into (16) yields

$$\begin{bmatrix} e_0 x_R[0] + e_1 x_R[1] - x_R[2] \\ e_0 x_I[0] + e_1 x_I[1] - x_I[2] \end{bmatrix}^T = \begin{bmatrix} 0 \\ 0 \end{bmatrix}^T \begin{bmatrix} \alpha_1 & \beta_1 \\ \alpha_2 & \beta_2 \end{bmatrix} = \begin{bmatrix} 0 \\ 0 \end{bmatrix}^T \quad (17)$$

Eq. (17) can be reduced to

$$\begin{bmatrix} x_R[0] & x_R[1] \\ x_I[0] & x_I[1] \end{bmatrix} \cdot \begin{bmatrix} e_0 \\ e_1 \end{bmatrix} = \begin{bmatrix} x_R[2] \\ x_I[2] \end{bmatrix} \quad (18)$$

Consequently, the coefficients e_k are obtained from

$$\begin{bmatrix} e_0 \\ e_1 \end{bmatrix} = \begin{bmatrix} x_R[0] & x_R[1] \\ x_I[0] & x_I[1] \end{bmatrix}^{-1} \begin{bmatrix} x_R[2] \\ x_I[2] \end{bmatrix} \quad (19)$$

Once the coefficients e_k are known, the two solutions of (14) are

$$z_{1,2} = e^{-\lambda \pm j 2\pi f \cdot \Delta t} = \frac{e_1 \pm j\sqrt{-e_1^2 - 4e_0}}{2} \quad (20)$$

The estimated fundamental frequency is given by

$$f = \frac{1}{2\pi \cdot \Delta t} \cos^{-1}\left(\frac{\mathrm{Re}(z_k)}{|z_k|}\right) = \frac{1}{2\pi \cdot \Delta t} \cos^{-1}\left(\frac{e_1}{2\sqrt{-e_0}}\right) \quad (21)$$

3. Performance Evaluation

3.1 Simulated Data

The simulation results presented in this section were all processed using Matlab. The sampling frequency was set to 7680 Hz or 128 samples per cycle in 60-Hz systems. The simulated data were pre-conditioned using a second-order Butterworth low-pass filter with a cutoff frequency of 600 Hz in order to reject high-frequency components and prevent aliasing errors. As mentioned in Section 2.1, the orthogonal decomposition used the variable window technique to enhance the ability of eliminating the harmonics. In the simulations, the variable window was updated after the estimated fundamental frequencies from one cycle were averaged.

In order to evaluate the performance of the algorithm, the results were compared to those obtained from the adaptive algorithm of Moore [16], which is one of the most useful techniques for estimating the fundamental frequency in power systems. Although complex Prony analysis theoretically requires three samples for Eq. (18), we obtained stable responses from single-cycle samples in the simulations. For comparison, the adaptive algorithm also used single-cycle samples to perform the gain compensation for calculating the best estimate of the fundamental frequency. As a result, the two algorithms used the same amount of samples.

3.2 Performance During Test Conditions

Amplitude modulation and harmonic tests were performed using simulated test signals. Three types of signals were considered: the ramp-up change given in (22), the ramp-down change given in (23), and the sinusoidal change given in (24):

$$\begin{cases} f[n] = f_0 & n < 0 \\ f[n] = f_0 + \dfrac{n}{W} & 0 \le n \le W \\ f[n] = f_0 + 1 & n > W \end{cases} \quad (22)$$

$$\begin{cases} f[n] = f_0 & n < 0 \\ f[n] = f_0 - \dfrac{n}{W} & 0 \le n \le W \\ f[n] = f_0 - 1 & n > W \end{cases} \quad (23)$$

$$\begin{cases} f[n] = f_0 & n < 0 \\ f[n] = f_0 + \sin(2\pi \dfrac{n}{W}) & 0 \le n \le W \\ f[n] = f_0 & n > W \end{cases} \quad (24)$$

where W is the number of samples per second.

1) Amplitude Modulation

For the amplitude modulation test, the signal described by Eq. (25) was provided as an input to both the proposed and adaptive algorithms,

$$x_1[n] = A[n] \sin(2\pi \frac{f[n]}{f_0} \frac{n}{N_0}) \quad (25)$$

where $\begin{cases} A[n] = 1.00 & n < 0 \\ A[n] = 1.00 + 0.50 \sin(2\pi \dfrac{n}{2W}) & 0 \le n \end{cases}$

Figs. 1 and 2 show the time responses of the two algorithms to ramp-up and sinusoidal changes in the signal, respectively. When the actual fundamental frequency was close to the nominal fundamental frequency, the simulation

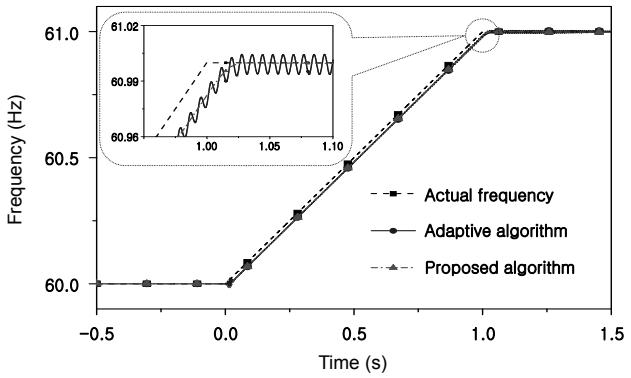

Fig. 1. Estimation of the ramp-up frequency change in the amplitude modulation test.

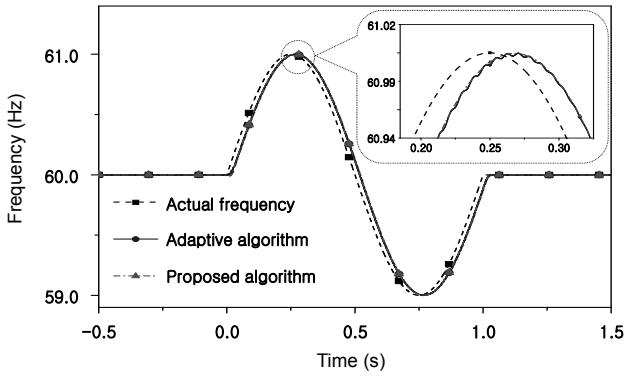

Fig. 2. Estimation of the sinusoidal frequency change in the amplitude modulation test.

results confirmed the good response of the two algorithms. However, when the actual fundamental frequency deviated from the nominal fundamental frequency, the adaptive algorithm produced some errors due to the amplitude modulation.

2) Harmonics

To investigate the influence of the harmonics, the following signal was considered:

$$\begin{aligned} x_2[n] = A[n]\sin(2\pi\frac{f[n]}{f_0}\frac{n}{N_0}) \\ +0.10\sin(2\pi\frac{2f[n]}{f_0}\frac{n}{N_0}) \\ +0.10\sin(2\pi\frac{3f[n]}{f_0}\frac{n}{N_0}) \\ +0.05\sin(2\pi\frac{5f[n]}{f_0}\frac{n}{N_0}) \end{aligned} \quad (26)$$

Figs. 3 and 4 reveal the ability of the proposed algorithm clearly. Although the adaptive algorithm produced considerable errors due to the harmonics as well as the amplitude

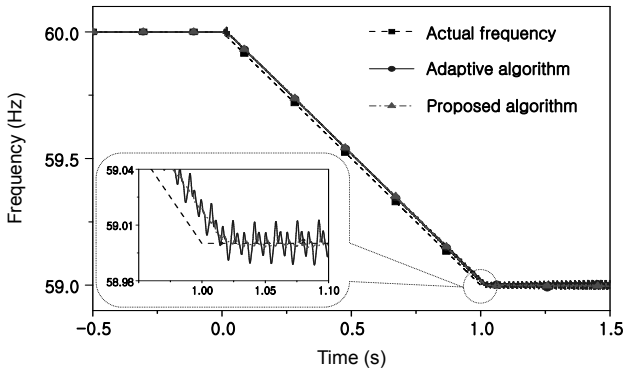

Fig. 3. Estimation of the ramp-down frequency change in the harmonic test.

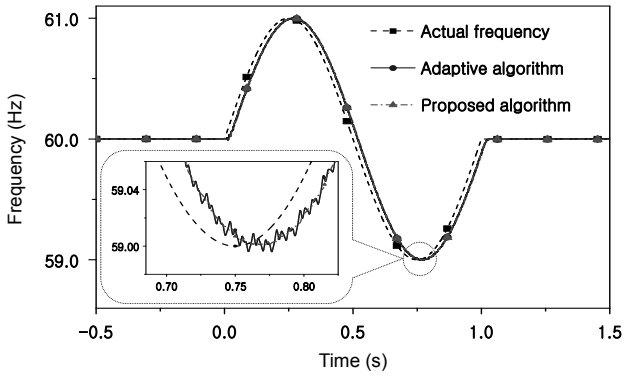

Fig. 4. Estimation of the sinusoidal frequency change in the harmonic test.

Table 1. Average estimation errors of the adaptive algorithm and the proposed algorithm

Test Condition	Frequency Change	Average Estimation Error (%)	
		Adaptive Algorithm	Proposed Algorithm
Amplitude Modulation	Ramp up	0.0010	0.0005
	Ramp down	0.0010	0.0006
	Sinusoidal	0.0025	0.0022
Harmonics	Ramp up	0.0043	0.0007
	Ramp down	0.0048	0.0021
	Sinusoidal	0.0034	0.0028

modulation, the time responses of the proposed algorithm were almost identical to those in the amplitude modulation test.

To evaluate the accuracy of the algorithms, the estimation error is calculated using the following equation:

$$\text{Error} = \frac{|\text{estimated frequency-reference frequency}|}{\text{reference frequency}} \times 100 \quad (27)$$

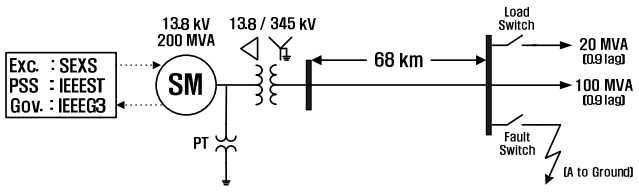

Fig. 5. Single machine power system under study.

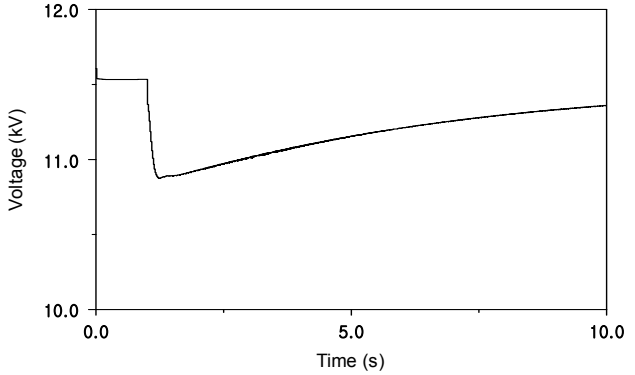

Fig. 6. Envelope of the generator terminal voltage when increasing the load by 20%.

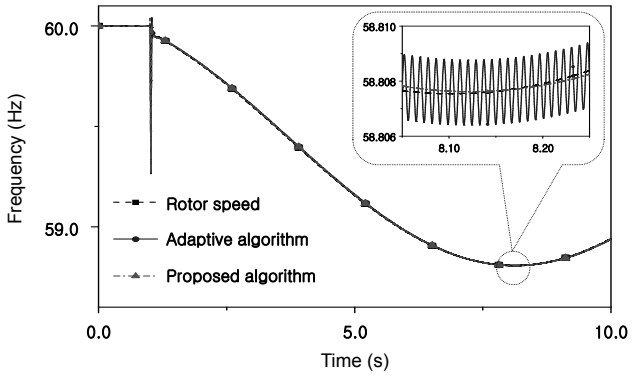

Fig. 7. Estimation of the fundamental frequency when increasing the load by 20%.

where the reference frequency is 132-sample delayed from the actual frequency, considering the delay time of the low-pass filter and the estimation algorithm. Table I summarizes the average values of estimation errors after one and a half cycles following the transient occurrence. Compared to the adaptive algorithm, which had an average estimation error between 0.0010 and 0.0048 %, the proposed algorithm estimated the frequency more accurately with an average estimation error between 0.0005 and 0.0028 %.

3.3 Performance in Power System Conditions

Dynamic conditions were investigated by using the Electromagnetic Transients Program (EMTP) to simulate the simple system shown in Fig. 5, consisting of a 200-MVA generator connected to a load, which was initially set to 100 MVA. Two kinds of dynamic conditions were considered: a load increase and single phase-to-ground faults. The zero crossing of a-phase voltage signal was chosen as reference angle.

1) Load Increase

The load switch shown in Fig. 5 was closed at time t = 1.00 s, thus loading the generator with an additional 20 MVA. This caused the amplitude of the generator terminal voltage to decrease instantaneously from 11.54kV to 10.87 kV, as shown in Fig. 6. The voltage waveform was processed by the two algorithms, and the estimated frequencies are depicted in Fig. 7 together with the actual frequency, which corresponds to the generator rotor speed obtained from the EMTP simulation.

The instantaneous change in the terminal voltage was responsible for a –0.75-Hz spike at 1.02 s in the estimated frequencies of the two algorithms. There is, of course, no corresponding instantaneous change in the rotor position and so the actual frequency did not vary in the same manner. Ignoring this effect, Fig. 7 clearly shows that the estimated frequencies of the two algorithms closely followed the actual frequency with an estimation delay of approximately 0.03 s. However, when magnifying the results shown in Fig. 7, it was found that the proposed algorithm delivered better results than the adaptive algorithm. Although the adaptive algorithm produced some oscillations due to the amplitude modulation of the terminal voltage, the proposed algorithm closely followed the actual frequency.

2) Single Phase-to-Ground Fault

The fault switch in Fig. 5 was closed at time t = 1.00 s and then opened at t = 1.10 s, creating an 'a' phase-to-ground 90° fault with a duration of 0.10 s. As shown in Fig. 8, the a-g 90° fault caused the amplitude of the generator terminal voltage to decrease instantaneously from 11.54 kV to 7.69 kV. This instantaneous decrease in the terminal voltage caused –3.61-Hz and –3.23-Hz spikes at 1.02 s in the estimated frequencies of the adaptive and proposed algorithms, respectively. After removing the fault at 1.10 s, the generator terminal voltage increased up to 12.18 kV and then settled to its initial value. Due to the instantaneous increase in the terminal voltage at 1.10 s, the estimated frequencies of the adaptive and proposed algorithms had 2.01-Hz and 2.56-Hz spikes at 1.13 s, respectively.

Similarly to a-g 90° fault, the fault switch was closed at time t = 1.00 s and then opened at t = 1.10 s, creating an a-g 0° fault. As shown in Fig. 10, the instantaneous decrease in the terminal voltage caused –3.30-Hz and –2.82-Hz spikes at 1.02 s in the estimated frequencies of the adaptive and proposed algorithms, respectively. After removing the fault at 1.10 s, the estimated frequencies of the adaptive and proposed algorithms had 1.85-Hz and 2.55-Hz spikes at 1.13 s, respectively.

Except for the spikes during the a-g faults, the estimated frequencies of the two algorithms closely followed the ac-

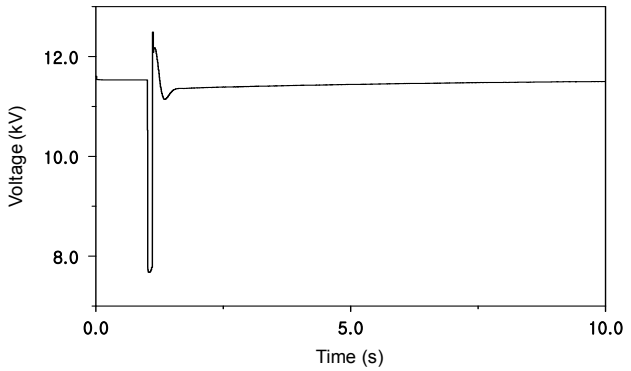

Fig. 8. Envelope of the generator terminal voltage when a single line-to-ground 90° fault occurs.

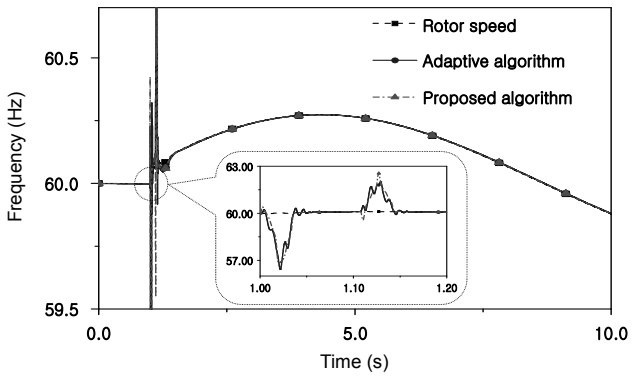

Fig. 9. Estimation of the fundamental frequency when a single phase-to-ground 90° fault occurs.

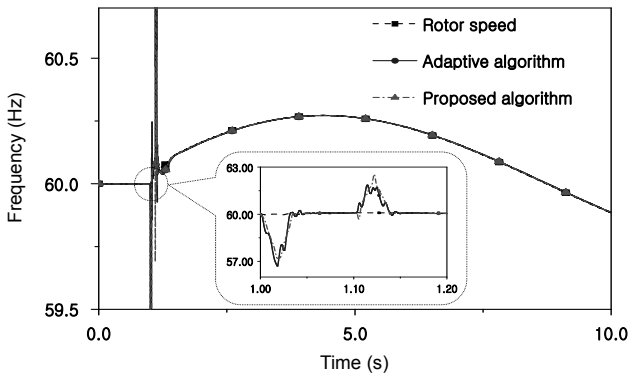

Fig. 10. Estimation of the fundamental frequency when a single phase-to-ground 0° fault occurs.

tual frequency. However, when magnifying the simulation results of Fig. 9 and Fig. 10, it was found that the estimated frequency of the proposed algorithm settled to the actual frequency after the fault inception and the fault elimination faster by approximately 0.01 s than that of the adaptive algorithm.

4. Conclusion

This paper describes a new algorithm for estimating the fundamental frequency of power system signals. The proposed algorithm consisted of orthogonal decomposition and a complex Prony analysis. The input signal was decomposed into two orthogonal components by using cosine and sine filters, and then a complex Prony analysis was used to estimate the fundamental frequency by approximating the cosine-filtered and sine-filtered signals in a complex exponential form.

To assess the performance of the algorithm, the results were compared to the adaptive algorithm using simulated test signals. The test results confirmed that the proposed algorithm could track the fundamental frequency accurately, even in the presence of amplitude modulation and harmonics.

Dynamic conditions in a single-machine power system were also investigated using the EMTP program. For an increase in load, the adaptive algorithm produced some oscillations due to the amplitude modulation of the terminal voltage; however the proposed algorithm closely followed the actual frequency. In case of single phase-to-ground faults, the estimated frequency of the proposed algorithm settled to the actual frequency faster than that of the adaptive algorithm. Therefore, the proposed algorithm is considered useful for estimating the fundamental frequency of power system signals.

Acknowledgements

This work was supported by the Human Resources Development of the Korea Institute of Energy Technology Evaluation and Planning (KETEP) grant funded by the Korea government Ministry of Knowledge Economy. (No. 2007-P-EP-HM-E-09-0000)

References

[1] M. M. Begovic, P. M. Djuric, S. Dunlap, A. G. Phadke, “Frequency tracking in power networks of harmonics,” *International Conference on Harmonics in Power Systems*, pp. 151-157, 1992.

[2] D. W. P. Thomas, M. S. Woolfson, “Evaluation of frequency tracking methods,” *IEEE Trans. Power Delivery*, Vol. 16, No. 3, pp. 367-371, 2001.

[3] A. Routray, A. K. Pradhan, K. P. Rao, “A novel Kalman filter for frequency estimation of distorted signals in power systems,” *IEEE Trans. Instrumentation and Measurement*, Vol. 51, No. 3, pp. 469-479, 2002.

[4] P. K. Dash, A. K. Pardhan, G. Panda, “Frequency estimation of distorted power system signals using extended complex Kalman filter,” *IEEE Trans. Power Delivery*, Vol. 14, No. 3, pp. 761-766, 1999.

[5] V. Kaura, V. Blasko, "Operation of a phase locked loop system under distorted utility conditions," *IEEE Trans. Industry Applications*, Vol. 33, No. 1, pp. 58-63, 1997.
[6] S.-K. Chung, "A phase tracking system for three phase utility interface inverters," *IEEE Trans. Power Electronics*, Vol. 15, No. 3, pp. 431-438, 2000.
[7] H. Karimi, M. Karimi-Ghartemani, M. R. Iravani, "Estimation of frequency and its rate of change for applications in power systems," *IEEE Trans. Power Delivery*, Vol. 19, No. 2, pp. 472-480, 2004.
[8] P. K. Dash, D. P. Swain, A. Routray, A. C. Liew, "An adaptive neural network approach for the estimation of power system frequency," *Electric Power Systems Research*, Vol. 41, No. 3, pp. 203-210, 1997.
[9] L. L. Lai, W. L. Chan, C. T. Tse, A. T. P. So, "Real-time frequency and harmonic evaluation using artificial neural networks," *IEEE Trans. Power Delivery*, Vol. 14, No. 1, pp. 52-59, 1999.
[10] M. S. Sachdev, M. M. Giray, "A least error squares technique for determining power system frequency," *IEEE Trans. Power Apparatus and Systems*, Vol. PAS-104, No. 2, pp. 437-444, 1985.
[11] M. M. Giray, M. S. Sachdev, "Off-nominal frequency measurement in electric power systems," *IEEE Trans. Power Delivery*, Vol. 4, No. 3, pp. 1573-1578, 1989.
[12] R. Chudamani, Krishna Vasudevan, C. S. Ramalingam, "Real-Time Estimation of Power System Frequency Using Nonlinear Least Squares," *IEEE Trans. Power Delivery*, Vol. 24, No. 3, pp. 1021-1028, 2009.
[13] V. V. Terzija, M. B. Djuric, B. D. Kovacevic, "Voltage phasor and local system frequency estimation using Newton-type algorithms," *IEEE Trans. Power Delivery*, Vol. 9, No. 3, pp. 1368-1374, 1994.
[14] T. Lobos, J. Rezmer, "Real-time determination of power system frequency," *IEEE Trans. Instrumentation and Measurement*, Vol. 46, No. 4, pp. 877-881, 1997.
[15] A. G. Phadke, J. S. Thorp, M. G. Adamiak, "A new measurement technique for tracking voltage phasors, local system frequency and rate of change of frequency," *IEEE Trans. Power Apparatus and Systems*, Vol. PAS-102, No. 5, pp. 1025-1038, 1983.
[16] P. J. Moore, R. D. Carranza, A. T. Johns, "A new numeric technique for high-speed evaluation of power system frequency," *IEE Proceedings - Generation Transmission and Distribution*, Vol. 141, No. 5, pp. 529-536, 1994.
[17] J. Z. Yang, C. W. Liu, "A precise calculation of power system frequency," *IEEE Trans. Power Delivery*, Vol. 16, No. 3, pp. 361-366, 2001.
[18] M. D. Kusljevic, "A simple recursive algorithm for frequency estimation," *IEEE Trans. Instrumentation and Measurement*, Vol. 53, No. 2, pp. 335-340, 2004.
[19] M. D. Kusljevic, "A simple recursive Algorithm for simultaneous magnitude and frequency estimation," *IEEE Trans. Instrumentation and Measurement*, Vol. 57, No. 6, pp. 1207-1214, 2008.
[20] D. Hart, D. Novosel, Yi Hu, B. Smith, M. Egolf, "A new frequency tracking and phasor estimation algorithm for generator protection," *IEEE Trans. Power Delivery*, Vol. 12, No. 3, pp. 1064-1073, 1997.

Soon-Ryul Nam received the B.S., M.S., and Ph.D. degrees in electrical engineering from Seoul National University, Seoul, Korea in 1996, 1998 and 2002, respectively. He is an assistant professor at Myongji University, Yongin, Korea.

Dong-Gyu Lee received the B.S., M.S. and Ph.D. degrees in electrical engineering from Myongji University, Korea, in 2002, 2004 and 2010, respectively. His main research interests are power system protection.

Sang-Hee Kang received the B.S., M.S. and Ph.D. degrees from Seoul National University, Korea in 1985, 1987 and 1993, respectively. He is a professor at Myongji University, Korea.

Seon-Ju Ahn received his B.S., M.S., and Ph.D. degrees in electrical engineering from Seoul National University, Seoul, Korea, in 2002, 2004, and 2009, respectively. He is a Full-Time Lecturer at Chonnam National University.

Joon-Ho Choi received the B.S., M.S. and Ph.D. degrees in Electrical Engineering from Soongsil University, Seoul, Korea in 1996, 1998 and 2002, respectively. He is an Associate Professor at Chonnam National University.